On the thermoelectric power factor of composites

A. Riss,[1, *] F. Garmroudi,[1] M. Parzer,[1] A. Pustogow,[1] T. Mori,[2, 3] and E. Bauer[1]
[1] *Institute of Solid State Physics, Technische Universität Wien, 1040 Vienna, Austria*
[2] *International Center for Materials Nanoarchitectonics (WPI-MANA),*
National Institute for Materials Science, Tsukuba 305-0044, Japan
[3] *University of Tsukuba, Tsukuba 305-8577, Japan*

To improve the performance of thermoelectric (TE) materials, a highly effective and widely implemented approach is to create multi-phase composites. These composites are designed to impede phononic heat transport, which accounts for the majority of thermal conductivity in conventional TE semiconductors. In 1999, Bergman and Fel reported that also the electronic properties, specifically the power factor, can be significantly enhanced in two-phase composites consisting of a highly-conducting, simple metal and a high-performance thermoelectric arranged in an optimal manner, sparking great experimental interest. In this work, we challenge the theoretical results of Bergman *et al.* and the conclusions drawn by them by using a simple and comprehensive model. We show that, while the improvement of the power factor is indeed extraordinary, the results lead to a misleading interpretation of the overall TE performance of the material. As a result, we argue that the power factor is not a suitable metric for evaluating multi-phase materials and composites and that the figure of merit zT should be used instead. Finally, we demonstrate that, nonetheless, the best TE composite always consists of a highly conductive metal and a high-performance thermoelectric in a serial configuration. This study presents an unintuitive yet auspicious approach to design high-performance TE composites with a large volume fraction of the metal component.

INTRODUCTION

In times of the steadily increasing energy consumption and prices, there is an increasing demand to use energy more efficiently. One promising solution are thermoelectric (TE) materials, which can convert waste heat to electrical energy by making use of the Seebeck effect. The efficiency of such a material is determined by the dimensionless figure of merit $zT = (S^2\sigma/\lambda)T$, which is composed of the Seebeck coefficient S (voltage per temperature gradient), the electrical conductivity σ and the thermal conductivity λ. Single-phase bulk compounds have been intensively studied over the past decades, resulting in very efficient state-of-the-art materials like Bi_2Te_3 [1, 2], PbTe [3–5], SiGe [6, 7], SnSe [8–10], Skutterudites [11–13] or Half-Heusler alloys [14–16] with large figures of merit. Driven by the requirement to decouple thermal and electrical transport in TE materials, more sophisticated strategies have been employed such as the synthesis of nano-wires [17, 18], thin films [19, 20] as well as nanostructured materials and multi-phase composites [21–24]. Apart from intrinsic property changes, such as a reduction of the lattice thermal conductivity from increased phonon scattering at the nano-, micro- and mesoscale defects and interfaces, a fundamental question arises for multi-phase composites: How and to what extent do the TE properties of the individual materials contribute towards the overall properties measured for the composite?

In the 1990s Bergman et al. theoretically showed that a „high-performance thermoelectric“ and a „benign metal“, *i.e.* a metal with high electrical and thermal conductivity, combined in a favourable spatial configuration, can boost the power factor $PF = S^2\sigma$ but not the figure of merit zT [25, 26], which restricts the potential of composites to a high power factor, when neglecting intrinsic property changes such as interface effects.

In this work, we elucidate the ongoing physics and conclude from a simplified model why the power factor is seemingly enhanced in such a system, in agreement with the calculations by Bergman and Fel [26]. Continuing the analysis of our results, we will show that the power factor enhancement is misinterpreted in these cases and distorts the performance of such composite materials. Ultimately, it can be shown by simple arguments that the power factor is not a good quantity and performance indicator when measuring a material consisting of at least two phases. This will hopefully shine a new light on the research of composites and rise the awareness of the ambivalent properties. Lastly, we highlight that, against common intuition, a two-phase heterostructure consisting of a thermoelectric with high zT and a perfect metal with high electrical and thermal conductivity is nonetheless the optimal thermoelectric composite.

THERMOELECTRIC PROPERTIES OF A SERIAL THERMOELECTRIC-METAL COMPOSITE

Bergman *et al.* calculated the overall thermoelectric properties of thermoelectric-metal composites for several different spatial configurations. They found that the power factor can be improved through either alternating serial slabs or a spherical structure where the metal is coated by the thermoelectric material. The latter is often a good approximation to more realistic structures, as stated by the authors. In this study, we will focus on the

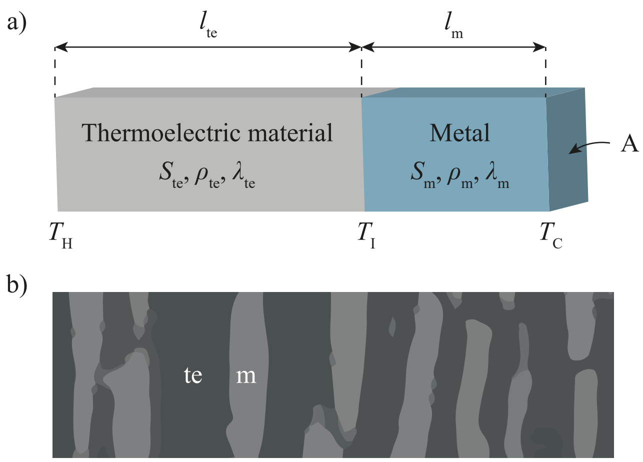

Figure 1: a) Schematic sketch of a serial connection of a thermoelectric material with the length l_{te} and a metal with the length l_{m}. Both materials have individual Seebeck coefficients S, electrical resistivities ρ and thermal conductivities λ. The hot temperature at the end of the thermoelectric material, the temperature at the interface and the cold temperature at the end of the metal are denoted as T_{H}, T_{I} and T_{C}, respectively. b) Sketch of the microstructure for a fictious thermoelectric composite material with a serial slab configuration.

slab configuration since it is simpler to model and provides more understanding about the origin of the changes in the performance.

Figure 1a illustrates the model used to calculate the properties. It is similar to the one used by Bergman *et al.*, but with only one interface instead of alternating slabs. When ignoring interface effects, as done in both studies, these two models are equivalent. Figure 1b provides a realistic example for the application of the model in a two-phase composite material.

Power factor

For a better understanding, we will first calculate the total power factor of a serial connection of a thermoelectric material and an ideal metal with $\rho_{\mathrm{m}} \to 0$ and therefore $\lambda_{\mathrm{m}} \to \infty$. From the benignity of the metal follows that the temperature at the interface $T_{\mathrm{I}} = T_{\mathrm{C}}$ and the whole temperature drops along the thermoelectric material. This leads to the thermovoltage U

$$U = S_{\mathrm{te}}\,(T_{\mathrm{H}} - T_{\mathrm{C}}) = S_{\mathrm{te}}\,\Delta T \ . \tag{1}$$

The total Seebeck coefficient S_{t} is calculated as $S_{\mathrm{t}} = U/\Delta T$, so

$$S_{\mathrm{t}} = S_{\mathrm{te}} \ . \tag{2}$$

The total resistance is only comprised of the resistance of the thermoelectric material due to the ideal conductivity of the metal. Thus, when calculating the resistivity, one obtains

$$\rho_{\mathrm{t}} = R_{\mathrm{te}}\,\frac{A}{l_{\mathrm{te}} + l_{\mathrm{m}}} = \rho_{\mathrm{te}}\,\frac{l_{\mathrm{te}}}{l_{\mathrm{te}} + l_{\mathrm{m}}} = \rho_{\mathrm{te}}\,\delta_{\mathrm{te}} \ , \tag{3}$$

with the volume fraction of the thermoelectric material δ_{te}.

While the Seebeck coefficient is not affected by the metal, the resistivity decreases due to $\delta_{\mathrm{te}} < 1$, resulting in an increase of the total power factor:

$$PF_{\mathrm{t}} = \frac{S_{\mathrm{t}}^2}{\rho_{\mathrm{t}}} = \frac{S_{\mathrm{te}}^2}{\rho_{\mathrm{te}}\,\delta_{\mathrm{te}}} = PF_{\mathrm{te}}\frac{1}{\delta_{\mathrm{te}}} \ . \tag{4}$$

When examining a more realistic scenario with finite conductivities, the temperature differences across the thermoelectric material and the metal, $\Delta T_{\mathrm{te}} = T_{\mathrm{H}} - T_{\mathrm{I}}$ and $\Delta T_{\mathrm{m}} = T_{\mathrm{I}} - T_{\mathrm{m}}$, can be calculated from the thermal conductance $C_i = \lambda_i A / l_i$ of both materials:

$$\Delta T_{\mathrm{te}} = \frac{C_{\mathrm{m}}}{C_{\mathrm{te}} + C_{\mathrm{m}}}\,\Delta T = \frac{l_{\mathrm{te}}\lambda_{\mathrm{m}}}{l_{\mathrm{m}}\lambda_{\mathrm{te}} + l_{\mathrm{te}}\lambda_{\mathrm{m}}}\,\Delta T \ , \tag{5}$$

$$\Delta T_{\mathrm{m}} = \frac{C_{\mathrm{te}}}{C_{\mathrm{te}} + C_{\mathrm{m}}}\,\Delta T = \frac{l_{\mathrm{m}}\lambda_{\mathrm{te}}}{l_{\mathrm{m}}\lambda_{\mathrm{te}} + l_{\mathrm{te}}\lambda_{\mathrm{m}}}\,\Delta T \ . \tag{6}$$

Unlike the previous case, the measured thermovoltage now has contributions from both the thermoelectric and the metal and is

$$\begin{aligned} U &= S_{\mathrm{te}}\,\Delta T_{\mathrm{te}} + S_{\mathrm{m}}\,\Delta T_{\mathrm{m}} \\ &= \frac{S_{\mathrm{te}}\,l_{\mathrm{te}}\lambda_{\mathrm{m}} + S_{\mathrm{m}}\,l_{\mathrm{m}}\lambda_{\mathrm{te}}}{l_{\mathrm{m}}\lambda_{\mathrm{te}} + l_{\mathrm{te}}\lambda_{\mathrm{m}}}\,\Delta T \ . \end{aligned} \tag{7}$$

This leads to

$$S_{\mathrm{t}} = \frac{S_{\mathrm{te}}\,l_{\mathrm{te}}\lambda_{\mathrm{m}} + S_{\mathrm{m}}\,l_{\mathrm{m}}\lambda_{\mathrm{te}}}{l_{\mathrm{m}}\lambda_{\mathrm{te}} + l_{\mathrm{te}}\lambda_{\mathrm{m}}} \ . \tag{8}$$

The total Seebeck coefficient can be written using a material-related quantity ε_λ, following the notation of our previous work about the thermoelectric properties of a film-substrate setup [27]:

$$S_{\mathrm{t}} = \frac{S_{\mathrm{te}} + \varepsilon_\lambda S_{\mathrm{m}}}{1 + \varepsilon_\lambda} \quad \text{with} \quad \varepsilon_\lambda = \frac{C_{\mathrm{te}}}{C_{\mathrm{m}}} = \frac{l_{\mathrm{m}}\lambda_{\mathrm{te}}}{l_{\mathrm{te}}\lambda_{\mathrm{m}}} \ . \tag{9}$$

Depending on the ratio between the individual thermal conductances, the total Seebeck coefficient lies between those of the thermoelectric material and the metal.

The finite conductivity further leads to a contribution of the metal to the total electrical resistivity. The measured resistance of the setup is

$$R_{\mathrm{t}} = R_{\mathrm{te}} + R_{\mathrm{m}} = \rho_{\mathrm{te}}\frac{l_{\mathrm{te}}}{A} + \rho_{\mathrm{m}}\frac{l_{\mathrm{m}}}{A} \tag{10}$$

and thus the electrical resistivity becomes

$$\rho_\mathrm{t} = R_\mathrm{t}\frac{A}{l} = \rho_\mathrm{te}\left(\delta_\mathrm{te} + \frac{\rho_\mathrm{m}}{\rho_\mathrm{te}}\left(1-\delta_\mathrm{te}\right)\right)\ , \tag{11}$$

which is a linear function depending on the volume fraction of the thermoelectric material. By introducing another quantity,

$$\varepsilon_\sigma = \frac{R_\mathrm{m}}{R_\mathrm{te}} = \frac{l_\mathrm{te}\rho_\mathrm{m}}{l_\mathrm{m}\rho_\mathrm{te}}\ , \tag{12}$$

Equation 11 can be further simplified to

$$\rho_\mathrm{t} = \rho_\mathrm{te}\delta_\mathrm{te}(1+\varepsilon_\sigma)\ . \tag{13}$$

Combining Equation 9 and Equation 11 leads to the total power factor of the system:

$$\begin{aligned} PF_\mathrm{t} &= \frac{S_\mathrm{t}^2}{\rho_\mathrm{t}} \\ &= \left(\frac{S_\mathrm{te}+\varepsilon_\lambda S_\mathrm{m}}{1+\varepsilon_\lambda}\right)^2 \frac{1}{\rho_\mathrm{te}\left(\delta_\mathrm{te}+\frac{\rho_\mathrm{m}}{\rho_\mathrm{te}}\left(1-\delta_\mathrm{te}\right)\right)}\ . \end{aligned} \tag{14}$$

The total power factor can also be written in terms of the individual power factors and the volume fraction of the thermoelectric material:

$$\begin{aligned} &PF_\mathrm{t}(\delta_\mathrm{te}) = \\ &\frac{\left(\sqrt{PF_\mathrm{te}} + \varepsilon_\lambda(\delta_\mathrm{te})\sqrt{\frac{\rho_\mathrm{m}}{\rho_\mathrm{te}}}\,\mathrm{sgn}\left(\frac{S_\mathrm{m}}{S_\mathrm{te}}\right)\sqrt{PF_\mathrm{m}}\right)^2}{\delta_\mathrm{te}\left(1+\varepsilon_\lambda(\delta_\mathrm{te})\right)^2\left(1+\varepsilon_\sigma(\delta_\mathrm{te})\right)} \end{aligned} \tag{15}$$

with the δ_te-dependent notation of the material-related quantities

$$\varepsilon_\varphi(\delta_\mathrm{te}) = \frac{\varphi_\mathrm{te}}{\varphi_\mathrm{m}}\left(\frac{1}{\delta_\mathrm{te}}-1\right)\Bigg|_{\varphi=\lambda,\sigma}\ . \tag{16}$$

A comparison between Equation 15 and the results of Bergman *et al.* can be observed in the Supplemental Material for three selected systems calculated by the authors. The remarkable agreement between the models validates our assumptions and underscores the informative value of the results presented here.

The presence of a local maximum in PF_t depends on whether the decrease in thermovoltage caused by the metal is overcompensated by the increase in electrical conductivity. The consequences of an enhanced power factor will be discussed later.

Figure of merit

Next, we will calculate the figure of merit zT, starting from an ideal metal.

The total thermal conductance C_t can be calculated, in accordance to the electrical conductance, as

$$\frac{1}{C_\mathrm{t}} = \frac{1}{C_\mathrm{te}} = \frac{l_\mathrm{te}}{\lambda_\mathrm{te}A} := \frac{l_\mathrm{te}+l_\mathrm{m}}{\lambda_\mathrm{t}A} \tag{17}$$

and thus

$$\lambda_\mathrm{t} = \lambda_\mathrm{te}\frac{1}{\delta_\mathrm{te}}\ . \tag{18}$$

The thermal conductivity increases with decreasing volume fraction of the thermoelectric material, similar to the electrical conductivity (see Equation 3). Combining Equation 18 and Equation 4 yields the total figure of merit

$$zT_\mathrm{t} = \frac{PF_\mathrm{t}}{\lambda_\mathrm{t}}T = \frac{PF_\mathrm{te}}{\lambda_\mathrm{te}}T = zT_\mathrm{te}\ . \tag{19}$$

The total thermal conductivity is modified, when the thermal conductivity of the metal is no longer infinite. It then becomes

$$\frac{1}{C_\mathrm{t}} = \frac{1}{C_\mathrm{te}} + \frac{1}{C_\mathrm{m}} = \frac{l_\mathrm{te}}{\lambda_\mathrm{te}A} + \frac{l_\mathrm{m}}{\lambda_\mathrm{m}A} = \frac{l_\mathrm{te}+l_\mathrm{m}}{\lambda_\mathrm{t}A} \tag{20}$$

$$\lambda_\mathrm{t} = \frac{\lambda_\mathrm{te}}{\delta_\mathrm{te}\left(1+\varepsilon_\lambda\right)}\ . \tag{21}$$

From that a convenient relation of the total figure of merit can by derived:

$$\begin{aligned} zT_\mathrm{t} &= \frac{PF_\mathrm{t}}{\lambda_\mathrm{t}}T \\ &= \frac{\left(\sqrt{zT_\mathrm{te}} + \sqrt{\varepsilon_\lambda\varepsilon_\sigma}\,\mathrm{sgn}\left(\frac{S_\mathrm{m}}{S_\mathrm{te}}\right)\sqrt{zT_\mathrm{m}}\right)^2}{\left(1+\varepsilon_\lambda\right)\left(1+\varepsilon_\sigma\right)}\ . \end{aligned} \tag{22}$$

As as example we calculated the thermoelectric power factor PF_t and the figure of merit zT_t for a composite consisting of a high-performance thermoelectric material, SnSe, mixed with elemental Ag as well as another thermoelectric material, PbTe (see Figure 2). The figure of merit in composites differs from the power factor in that there is never a local maximum when forming a composite, *i.e.* zT_t of the composite always ranges between the values obtained for the pristine materials. A striking feature in Figure 2 is that in case of a thermoelectric-metal composite the figure of merit remains nearly constant even at very low volume fractions of the thermoelectric material due to the exceptional electrical and thermal conductivity of the metal. This can be explained by the fact that in a serial configuration most of the temperature difference occurs across the thermoelectric material, preserving the thermovoltage, while the balance between increased electrical and thermal conductivity maintains zT. Deviation from ideal conduction in the metal is the only factor that decreases the overall zT_t (see Equation 19).

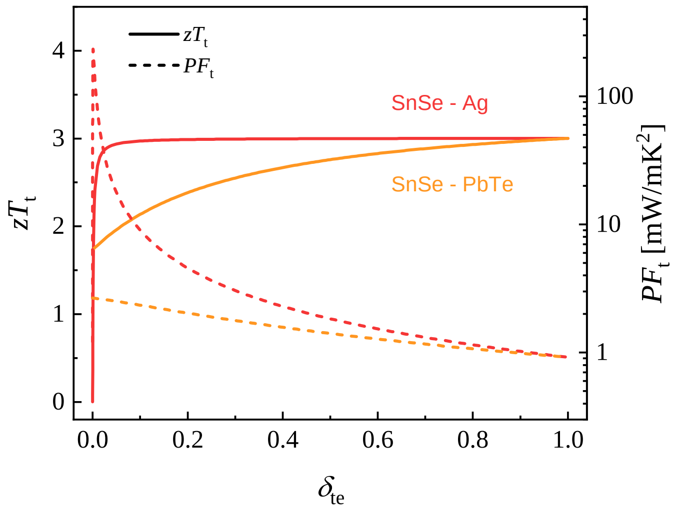

Figure 2: Total figure of merit zT_t (solid lines) and power factor (dashed lines) of a serial connection of polycrystalline SnSe and Ag (red line) and PbTe (orange line) in dependence of the volume fraction δ_{te} of SnSe, calculated from Equation 15 and Equation 22. The values of all materials' properties were taken from literature [4, 10, 28–30].

In contrast to that, for a thermoelectric-thermoelectric composite both PF_t and zT_t show a more linear behavior as a function of the volume fraction, revealing the inferiority of such systems compared to single thermoelectric materials.

COMPARISON BETWEEN POWER FACTOR AND POWER OUTPUT

To further elucidate the meaning of the power factor of composites, we will compare PF_t, zT_t and the power output for the three different systems comprised of the archetypical thermoelectric material Bi_2Te_3 and elemental Al, as depicted in Figure 3a. These include a pure thermoelectric (I), a thermoelectric-metal composite (II) as well as the thermoelectric with reduced length (III). The maximum possible power output for a given given temperature difference is [32]

$$P_t^{max} = \frac{PF_t A \Delta T^2}{4l} \ . \tag{23}$$

The total power factor, figure of merit and power output are shown in Figure 3b.

The Bi_2Te_3-Al composite (II) outperforms pure Bi_2Te_3 (I) in terms of power factor and power output. Incorporating metal components into the thermoelectric material improves the power generated by reducing the total resistance while the Seebeck coefficient S is almost unaffected, thereby seemingly decoupling S and σ, two transport properties which are usually difficult to enhance simultaneously [33]. However, a comparison between systems II and III shows that when comparing both systems at the same volume fraction of the active TE component, the power output is higher without the metal despite the fact that the metal-composite has a seemingly much higher power factor. Thus, the enhancement of the power factor as described by Bergman and Fel and also the present study merely results from a favourable yet nonsensical comparison of two materials with different volume fractions of the active TE component. We emphasize that this illustrates that the power factor is no longer a valid

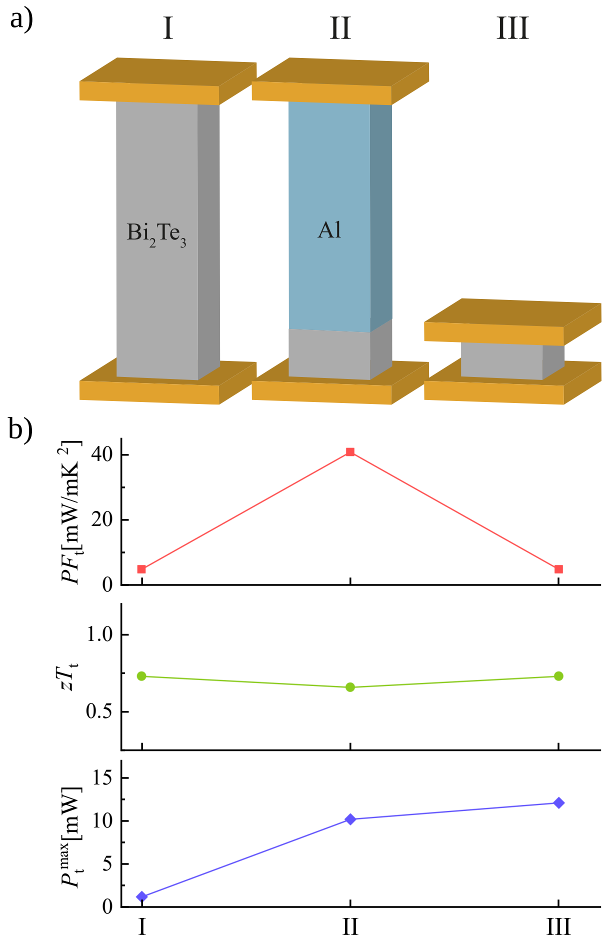

Figure 3: a) Sketch of the three systems compared in the text with respect to their thermoelectric performance. I: (I-doped) Bi_2Te_3, II: Bi_2Te_3-Al composite with $\delta_{te} = 0.1$, III: Bi_2Te_3 with reduced length similar to system II. b) Power factor, figure of merit and maximum power output for all three systems. The power output was calculated using $l = 1\,\text{cm}$, $A = 1\,\text{mm}^2$, $T = 300\,\text{K}$ and $\Delta T = 100\,\text{K}$. For the sake of simplicity, all thermoelectric properties were taken at 300 K [2, 28, 29, 31].

indicator for TE device performance in composite materials. Since a large PF neither indicates a higher zT nor a higher power output in such composites, the power factor becomes a meaningless parameter for evaluating materials. Only in fixed-length setups, if power output is more critical than efficiency, the use of composites can significantly increase power output by reducing the volume fraction of the thermoelectric material and lowering the resistance.

Another potential application for thermoelectric materials with high power factors is the so-called active Peltier cooling, which combines traditional heat conduction with the Peltier effect to enhance cooling capabilities [34]. In this context, a large thermal conductivity and power factor are desired to maximize the effective thermal conductivity λ_{eff}:

$$\lambda_{\mathrm{eff}} = \left(\lambda + \frac{PF T_{\mathrm{H}}^2}{2\Delta T}\right) , \tag{24}$$

with the temperature of the hot side T_{H}. Active cooling does indeed looks like a promising application when composites are compared to conventional materials (see Supplemental Materials).

However, it is important to examine the macroscopic quantity of the actual cooling power, as the high power factor can be misleading and give a false impression of the performance. A closer look at the cooling power,

$$\frac{dQ}{dt} = \lambda_{\mathrm{eff}} \frac{A}{l} \Delta T = \left(L + \frac{S^2 T_{\mathrm{H}}^2}{2R\Delta T}\right) \Delta T , \tag{25}$$

reveals the inferiority of composites to pure thermoelectrics. Adding a simple metal to the thermoelectric material slightly decreases the thermal conductance and increases the resistance, thus reducing the cooling power. Conversely, substituting part of the thermoelectric material with a metal increases the thermal conductance and reduces the resistance, enhancing the cooling power – but then again, removing the entire metal further increases the efficiency.

THE BEST COMPOSITE

Before exploring the potential applications of composites, it is important to acknowledge that the formulas used to predict the thermoelectric performance are subject to ideal conditions and may not accurately reflect real-world scenarios. This is because they do not account for the impact of external factors such as contact resistances and inter-phase scattering. As a result, the actual performance may differ from predicted values. On the other hand, more realistic, disordered composites can often be approximated by spherical structures, which show the same tendency as parallel slabs [26]. Thus, the following statements should be valid in many cases.

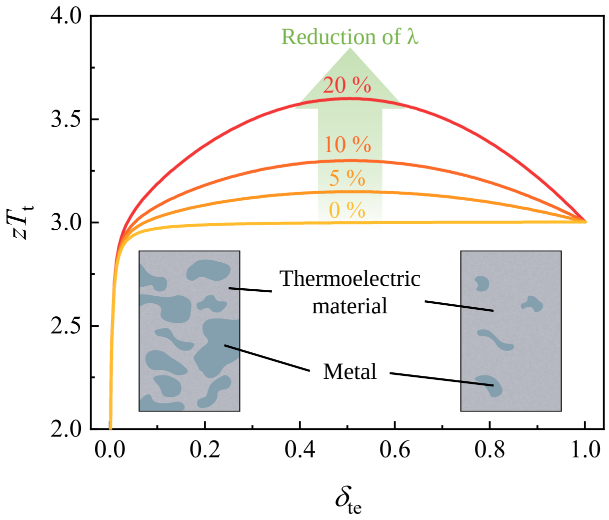

Figure 4: Figure of merit zT_{t} of a SnSe-Ag composite for different reductions of lambda due to increased scattering on the metallic structures. The reduction was calculated from a simple δ_{te}-dependent relation, $\lambda_{\mathrm{t}}^{\mathrm{red}} = \lambda_{\mathrm{t}}/[1 + a\delta_{\mathrm{te}}(1 - \delta_{\mathrm{te}})]$, with a chosen such that the reduction equals 5 %, 10 % and 20 % for $\delta_{\mathrm{te}} = 0.5$.

As we have shown in this work, an enhancement of the thermoelectric properties due to a smart combination of a high-performance thermoelectric and a simple metal in a serial configuration is not possible without intrinsic property changes of the individual materials comprising the composite, such as interface effects. When considering the significant impact of these secondary effects on the properties of real composite materials, and the frequent use of composites to improve the figure of merit, it prompts the question of which materials are best suited for making composites.

As can be seen in Figure 2 the total figure of merit zT_{t} stays almost constant down to a few percent of the volume fraction of the TE material when a simple metal is used as the second material. This opens a gigantic playground to reduce the lattice thermal conductivity via increased boundary scattering, as sketched in Figure 4. Although the reduction of the thermal conductivity is shown for an oversimplified δ_{te} relation, it is clearly visible that scattering of phonons with long mean free paths on mesoscale-sized metallic structures will have a positive effect on the performance [23]. Hence, adding a non-soluble and highly conducting metal is a cheap and profitable strategy to achieve a larger figure of merit.

CONCLUSION

We recalculated the results of Bergman et Fel [26] from a simple model while avoiding any approximations. Our results shed a new light on the origin of the extreme power factor values derived for composites, which are caused by a drastic reduction of the resistance while the thermovoltage only changes moderately. We further elucidated the misleading meaning of the power factor in such multi-phase systems by comparing measurable macroscopic quantities such as the power output to pure thermoelectric materials. We strongly advise using the robust and error-resistant figure of merit zT when comparing the performance of composite systems to single-phase thermoelectric materials. Lastly, we showed that, in theory, the best thermoelectric composite consists of a high-zT thermoelectric and a simple metal with maximal thermal and electrical conductivity.

ACKNOWLEDGEMENTS

Financial support for the research in this paper was granted by the Japan Science and Technology Agency (JST) programs MIRAI, JPMJMI19A1.

---

* alexander.riss@tuwien.ac.at

[1] L. Yang, Z.-G. Chen, M. Hong, G. Han, and J. Zou, Enhanced thermoelectric performance of nanostructured bi2te3 through significant phonon scattering, ACS applied materials & interfaces **7**, 23694 (2015).

[2] I. T. Witting, T. C. Chasapis, F. Ricci, M. Peters, N. A. Heinz, G. Hautier, and G. J. Snyder, The thermoelectric properties of bismuth telluride, Advanced Electronic Materials **5**, 1800904 (2019).

[3] J. P. Heremans, V. Jovovic, E. S. Toberer, A. Saramat, K. Kurosaki, A. Charoenphakdee, S. Yamanaka, and G. J. Snyder, Enhancement of thermoelectric efficiency in pbte by distortion of the electronic density of states, Science **321**, 554 (2008).

[4] Y. Pei, X. Shi, A. LaLonde, H. Wang, L. Chen, and G. J. Snyder, Convergence of electronic bands for high performance bulk thermoelectrics, Nature **473**, 66 (2011).

[5] Y. Pei, A. LaLonde, S. Iwanaga, and G. J. Snyder, High thermoelectric figure of merit in heavy hole dominated pbte, Energy & Environmental Science **4**, 2085 (2011).

[6] G. Joshi, H. Lee, Y. Lan, X. Wang, G. Zhu, D. Wang, R. W. Gould, D. C. Cuff, M. Y. Tang, M. S. Dresselhaus, *et al.*, Enhanced thermoelectric figure-of-merit in nanostructured p-type silicon germanium bulk alloys, Nano letters **8**, 4670 (2008).

[7] X. Wang, H. Lee, Y. Lan, G. Zhu, G. Joshi, D. Wang, J. Yang, A. Muto, M. Tang, J. Klatsky, *et al.*, Enhanced thermoelectric figure of merit in nanostructured n-type silicon germanium bulk alloy, Applied Physics Letters **93**, 193121 (2008).

[8] L.-D. Zhao, S.-H. Lo, Y. Zhang, H. Sun, G. Tan, C. Uher, C. Wolverton, V. P. Dravid, and M. G. Kanatzidis, Ultralow thermal conductivity and high thermoelectric figure of merit in snse crystals, nature **508**, 373 (2014).

[9] L.-D. Zhao, C. Chang, G. Tan, and M. G. Kanatzidis, Snse: a remarkable new thermoelectric material, Energy & Environmental Science **9**, 3044 (2016).

[10] C. Zhou, Y. K. Lee, Y. Yu, S. Byun, Z.-Z. Luo, H. Lee, B. Ge, Y.-L. Lee, X. Chen, J. Y. Lee, *et al.*, Polycrystalline snse with a thermoelectric figure of merit greater than the single crystal, Nature materials **20**, 1378 (2021).

[11] C. Uher, Skutterudites: Prospective novel thermoelectrics, in *Semiconductors and semimetals*, Vol. 69 (Elsevier, 2001) pp. 139–253.

[12] X. Shi, J. Yang, J. R. Salvador, M. Chi, J. Y. Cho, H. Wang, S. Bai, J. Yang, W. Zhang, and L. Chen, Multiple-filled skutterudites: high thermoelectric figure of merit through separately optimizing electrical and thermal transports, Journal of the American Chemical Society **133**, 7837 (2011).

[13] G. Rogl, A. Grytsiv, K. Yubuta, S. Puchegger, E. Bauer, C. Raju, R. Mallik, and P. Rogl, In-doped multifilled n-type skutterudites with zt= 1.8, Acta Materialia **95**, 201 (2015).

[14] C. Fu, T. Zhu, Y. Liu, H. Xie, and X. Zhao, Band engineering of high performance p-type fenbsb based half-heusler thermoelectric materials for figure of merit zt¿ 1, Energy & Environmental Science **8**, 216 (2015).

[15] C. Fu, S. Bai, Y. Liu, Y. Tang, L. Chen, X. Zhao, and T. Zhu, Realizing high figure of merit in heavy-band p-type half-heusler thermoelectric materials, Nature communications **6**, 8144 (2015).

[16] W. G. Zeier, J. Schmitt, G. Hautier, U. Aydemir, Z. M. Gibbs, C. Felser, and G. J. Snyder, Engineering half-heusler thermoelectric materials using zintl chemistry, Nature Reviews Materials **1**, 1 (2016).

[17] A. L. Prieto, M. S. Sander, M. S. Martin-Gonzalez, R. Gronsky, T. Sands, and A. M. Stacy, Electrodeposition of ordered bi2te3 nanowire arrays, Journal of the American Chemical Society **123**, 7160 (2001).

[18] O. Rabina, Y.-M. Lin, and M. S. Dresselhaus, Anomalously high thermoelectric figure of merit in bi 1- x sb x nanowires by carrier pocket alignment, Applied Physics Letters **79**, 81 (2001).

[19] R. Venkatasubramanian, E. Siivola, T. Colpitts, and B. O'quinn, Thin-film thermoelectric devices with high room-temperature figures of merit, Nature **413**, 597 (2001).

[20] B. Hinterleitner, I. Knapp, M. Poneder, Y. Shi, H. Müller, G. Eguchi, C. Eisenmenger-Sittner, M. Stöger-Pollach, Y. Kakefuda, N. Kawamoto, *et al.*, Thermoelectric performance of a metastable thin-film heusler alloy, Nature **576**, 85 (2019).

[21] W. Kim, J. Zide, A. Gossard, D. Klenov, S. Stemmer, A. Shakouri, and A. Majumdar, Thermal conductivity reduction and thermoelectric figure of merit increase by embedding nanoparticles in crystalline semiconductors, Physical review letters **96**, 045901 (2006).

[22] Z. Xiong, X. Chen, X. Zhao, S. Bai, X. Huang, and L. Chen, Effects of nano-tio2 dispersion on the thermoelectric properties offilled-skutterudite ba0. 22co4sb12, Solid State Sciences **11**, 1612 (2009).

[23] K. Biswas, J. He, I. D. Blum, C.-I. Wu, T. P. Hogan, D. N. Seidman, V. P. Dravid, and M. G. Kanatzidis, High-performance bulk thermoelectrics with all-scale hierarchical architectures, Nature **489**, 414 (2012).

[24] F. Delorme, P. Diaz-Chao, E. Guilmeau, and F. Giovannelli, Thermoelectric properties of ca3co4o9–co3o4 composites, Ceramics International **41**, 10038 (2015).

[25] D. J. Bergman and O. Levy, Thermoelectric properties of a composite medium, Journal of Applied Physics **70**,

6821 (1991).

[26] D. J. Bergman and L. G. Fel, Enhancement of thermoelectric power factor in composite thermoelectrics, Journal of Applied physics **85**, 8205 (1999).

[27] A. Riss, M. Stöger, M. Parzer, F. Garmroudi, N. Reumann, B. Hinterleitner, T. Mori, and E. Bauer, Criteria for erroneous substrate contribution to the thermoelectric performance of thin films, Phys. Rev. Appl. **19**, 054024 (2023).

[28] C. Ho, M. Ackerman, K. Wu, S. Oh, and T. Havill, Thermal conductivity of ten selected binary alloy systems, Journal of Physical and Chemical Reference Data **7**, 959 (1978).

[29] C. Y. Ho, M. Ackerman, K. Wu, T. Havill, R. Bogaard, R. Matula, S. Oh, and H. James, Electrical resistivity of ten selected binary alloy systems, Journal of physical and chemical reference data **12**, 183 (1983).

[30] C. Ho, R. Bogaard, T. Chi, T. Havill, and H. James, Thermoelectric power of selected metals and binary alloy systems, Thermochimica acta **218**, 29 (1993).

[31] R. J. Gripshover, J. B. VanZytveld, and J. Bass, Thermopower of pure aluminum, Physical Review **163**, 598 (1967).

[32] J. Chen, Z. Yan, and L. Wu, The influence of thomson effect on the maximum power output and maximum efficiency of a thermoelectric generator, Journal of applied physics **79**, 8823 (1996).

[33] G. J. Snyder and E. S. Toberer, Complex thermoelectric materials, Nature materials **7**, 105 (2008).

[34] M. Adams, M. Verosky, M. Zebarjadi, and J. Heremans, Active peltier coolers based on correlated and magnon-drag metals, Physical Review Applied **11**, 054008 (2019).